

Correlation Analysis of Statistical Microstructure Descriptors with Micromechanical Responses of Particulate Composite Materials

*Yeonghwan Kim¹⁾ and Gunjin Yun²⁾

^{1), 2)} *Department of Mechanical & Aerospace Engineering, Seoul National University, Seoul 08826, Korea*

¹⁾ gunjin.yun@snu.ac.kr

ABSTRACT

In this paper, correlation analysis of statistical microstructure descriptors and effective stiffnesses of particulate composites was demonstrated. Two-point correlation function and various morphological properties were extracted from synthetically generated RVE with different particle size and volume fraction. Effective stiffnesses of the periodic RVE were computed by the FE-based computational homogenization method. Correlations between the microstructure variables and effective stiffnesses were evaluated. Investigating correlations of the effective stiffness properties with the microstructure information, critical design variables for the particulate composite materials can be identified.

1. INTRODUCTION

Applications of the state-of-the-art composite materials in aerospace, automotive, construction industries have ever been growing. Recently, researches on novel strategies for design of composite materials are actively undergoing. For composite materials, microstructures and constituents' properties can be tailored through optimization of processing variables to meet a targeted performance in the structural level. To realize such paradigm by hierarchical design of composite materials, a reference relationship of process-structure-property-performance needs to be identified (Olson 1997, McDowell and Olson 2008). To draw the structure-property relationship, keys are to identify critical microstructure descriptors and determine effective properties of the random microstructure through the homogenization technique.

Various analytical and computational homogenization methods are widely used for computing effective stiffnesses (Yuan and Fish 2008, Charalambakis 2010).

¹⁾ Graduate Student

²⁾ Corresponding author, Professor, Department of Mechanical & Aerospace Engineering, Seoul National University, Gwanak-gu Gwanak-ro 1, Building 301 Room 1308, Seoul, 08826, South Korea, Tel)+82-2-880-8302

However, it still needs improvement on numerical techniques for homogenization (Akpyomare *et al.* 2017). Relatively more active researches focus on microstructure descriptors (Fullwood *et al.* 2010, Xu *et al.* 2014, Xu *et al.* 2017). For example, spectral representation of microstructure distribution functions was proposed (Fullwood *et al.* 2010). Recently, a principal component analysis (PCA)-based descriptor was also suggested that can allow analytical approximation of the structure-property relationship (Xu *et al.* 2017). However, no single tractable approach exists that generally correlates complex microstructure with properties. Analytical approximations for the relationship are exorbitantly scarce.

The motivation of this study is to design microstructures of particulate composite materials that satisfy the targeted properties at the microscale. Toward the final goal, structure-property correlations of particulate composites was evaluated first by an efficient computational homogenization and microstructure analysis of heterogeneous periodic representative volume element (RVE). The two-point correlation function (TPCF) is the most widely used second-order descriptor. Therefore, TPCF was computed. In addition, morphological features of the microstructures were also computed such as principal moment of inertia, radius of gyration in the principal direction, surface area, local volume fraction, and the shape index. For correlation analysis, volume fraction and particle sizes were varied and effective stiffnesses of the RVE under periodic boundary condition (PBC) were computed.

In the following section, a statistical microstructure descriptor and morphological properties were introduced. In Section 3, an efficient computational homogenization method was proposed. The proposed method can take non-matching finite element meshes between facing surfaces where PBC is imposed. In Section 4, RVE containing randomly distributed particles were analyzed and their results were presented. Finally, conclusions were included in Section 6 along with future research directions.

2. STATISTICAL MICROSTRUCTURE DESCRIPTORS

For two-phase particulate composites, volume fraction and size of particles are main design variables since effective material properties could dramatically change depending on the variables. In special materials such as mechanoluminescence (ML) composites, the stress intensity in the particles is a critical physical variable, which is closely related to morphological shapes. For the reason, we present a morphology analysis method on the particles.

2.1 Two-Point Correlation Function

In this section, the TPCF is introduced (Tewari *et al.* 2004). ϕ_i ($i=1$ and 2) indicates two phases of particulate composites. On a microstructure image, two points (S_1 and S_2) expressed by two position vectors (r_1 and r_2) are randomly selected. Then TPCF is a measure of likelihood of landing of each point S_1 and S_2 in a particular phase (Torquato 2002). It is a function of the magnitude of the vector ($r=|r_2-r_1|$). Numerically TPCF is calculated as follows (Ghazavizadeh *et al.* 2012)

$$P_{ij}(\mathbf{r}) = \frac{N_{ij}}{N} \Big|_{N \rightarrow \infty} [\mathbf{r} = \mathbf{r}_2 - \mathbf{r}_1, (S_1 \in \phi_i) \cap (S_2 \in \phi_j)] \quad (1)$$

where N_{ij} is the number of vectors with the beginning in phase ϕ_i and the end in phase ϕ_j . In two limiting cases where the magnitude (r) goes to either zero or infinity, the TPCF is related with volume fraction (v_i and v_j) of each phase as

$$\begin{aligned} \lim_{r \rightarrow 0} P_{ij}(r) &= v_i (i = j), \\ \lim_{r \rightarrow 0} P_{ij}(r) &= 0 (i \neq j), \\ \lim_{r \rightarrow \infty} P_{ij}(r) &= v_i v_j \end{aligned} \quad (2)$$

2.2 Morphology Analysis of Particles

Microstructure images such as SEM or micro-computed tomography (μ -CT) images consist of digitized three-dimensional (3D) voxels with binary indices or finite grey levels. Thus, based on the 3D voxel model, morphological features of the particles such as volume, surface area, the second moment of inertia, principal radius of gyration and shape index of particles are obtained.

A criterion for separating a particle from others is applied (Teranishi *et al.* 2016) if neighboring voxels share a surface, they are included in the same particle. However, if they do not share a surface and just share edge, vertex or nothing, they belong to separated particles. Volume of a particle (V) is calculated by multiplying the number of voxels (n) in the particle and a unit volume (V_0) of a voxel. The second moment of inertia is calculated by

$$I_{ij} = V_0 \sum_{m=1}^n (x_i^m - \bar{X}_i)(x_j^m - \bar{X}_j) \quad \text{where} \quad \bar{X}_i = \frac{1}{n} \sum_{m=1}^n x_i^m \quad (3)$$

where x_i^m is the coordinate of the center of m -th voxel and \bar{X}_i is the geometrical center of a particle in Cartesian coordinate system ($i=1,2,3$).

The principal second moments of inertia (I_1, I_2 and I_3) are eigenvalues of I_{ij} . The principle radius of gyration is defined as

$$r_i = \sqrt{I_i/V} \quad \text{where} \quad r_1 > r_2 > r_3 \quad (4)$$

The aspect ratio (a) of a particle is defined as

$$a = r_3/r_1 \quad (5)$$

The inclination of a particle of our interest is described by an angle (θ) between the first principal direction and loading axis. Then the surface area is calculated as follows

$$S = \sum_{m=1}^n S_u (6 - n_{nb}^m) \quad (6)$$

Where S_u is the area of one side surface of a voxel; and n_{nb}^m is the number of neighboring voxels around m -th voxel. Therefore, the total surface area of an isolated voxel is $6S_u$. Then the shape index (β) is also defined as

$$\beta = V/(Sr_1) \quad (7)$$

where S is the surface area of a particle. Based on these morphological features, local volume fractions can be evaluated within a spherical volume having a specific radius.

3. FE-BASED COMPUTATIONAL HOMOGENIZATION

FE-based computational homogenization method can easily handle heterogeneous RVE with periodic microstructure of particulate composites compared to other analytical homogenization methods. However, special numerical care is required to apply periodic kinematic boundary conditions on non-matching meshes.

3.1 Periodic Boundary Condition for Non-Matching Meshes

The general constraint equation for periodic boundary condition (PBC) is expressed as (Shahzamanian *et al.* 2014)

$$u_i^{j-} - u_i^{j+} - \Delta L_x \epsilon_{i1} - \Delta L_y \epsilon_{i2} - \Delta L_z \epsilon_{i3} = 0 \quad (8)$$

where u_i^{j-} is the displacement of the slave node and u_i^{j+} is the displacement of the master node. i is x , y and z in Cartesian coordinate system. ΔL_i is the relative distance between two nodes (Fig. 1). The nodes on the RVE boundary are grouped by their locations, that is, surface nodes, edge nodes, and vertex nodes because their relative distances are different depending on the group and this grouping prevents nodes from being over-constrained (Shahzamanian *et al.* 2014).

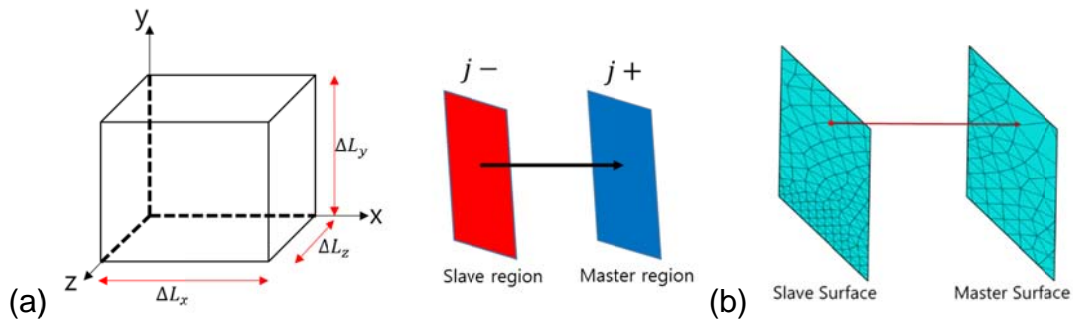


Fig. 1 (a) Notation of PBC kinematic equation and (b) non-matching meshes

Eq. (8) changes depending on the region where nodes are located: surfaces, edges, and vertices. For surface nodes, there are three pairs of surfaces (i.e. three equations). For edge nodes, the relative distance vector between nodes on facing edges have two components, that is, x - y , y - z or x - z . Therefore, there are six pairs of edges (i.e. six equations). In the case of vertex nodes, the relative distance vector between nodes on facing vertices has three components. Therefore, there are four pairs of vertices (i.e. four equations).

For finite element analysis, ABAQUS was used where the PBC kinematic equations are defined by “* equation” command. However, “* equation” can be used only if nodes on facing surfaces, edges and vertices are in one-to-one match. Therefore, a special numerical interpolation technique was implemented.

To resolve the PBC issue in ABAQUS for non-matching meshes, nodes in the slave region are projected onto the master region. All slave nodes fall into one of the elements on the master surface. Depending on the slave node position, displacements of the slave nodes are constrained to nodal displacements of the element as

$$u_i^{j-} - \sum_{k=1}^n [W_k u_k^{j+}] - \Delta L_x \epsilon_{i1} - \Delta L_y \epsilon_{i2} - \Delta L_z \epsilon_{i3} = 0 \quad (9)$$

where weighting factors W_k are calculated by the shape functions of the element; and n is the number of nodes of the element. These weighting factors are specified in “* equation” with the associated nodes.

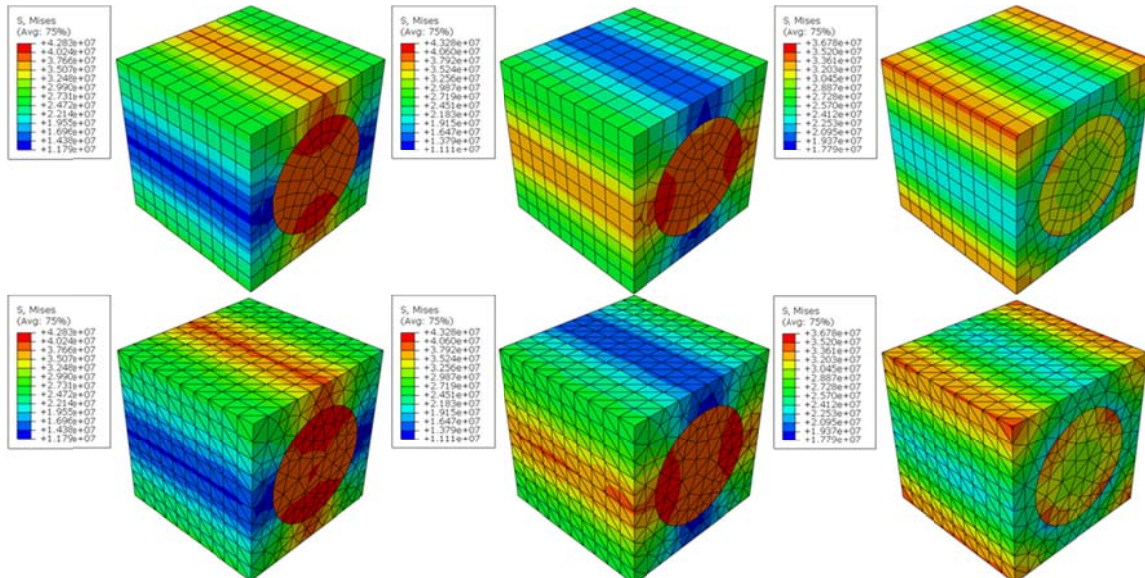


Fig. 2 von Mises stresses for matching hexahedron elements (Top) and non-matching tetrahedron elements (bottom) under unit shear strains

As shown in Fig. 2, stresses under PBC applied for non-matching meshes were reasonably close to those for matching meshes. Homogenized engineering constants were compared for both cases.

Table 1 Comparisons of effective engineering constants for matching and non-matching meshes (unit for E and G: MPa)

	Matching	Non-matching		Matching	Non-matching		Matching	Non-matching
E_1	56.60	56.60	ν_{12}	0.2657	0.2656	G_{12}	17.81	17.88
E_2	46.56	46.79	ν_{13}	0.2656	0.2656	G_{13}	17.82	17.88
E_3	46.57	46.80	ν_{23}	0.2849	0.2822	G_{23}	16.41	16.50

4. MICROSTRUCTURE ANALYSIS OF PARTICULATE COMPOSITES

The particles are shaped in the form of icosahedron as shown in Fig. 3(a). For subsequent analysis, nine different RVEs were generated synthetically with three volume fractions (0.15, 0.25, 0.3) and three particle sizes (2, 3.5, 5.0 unit).

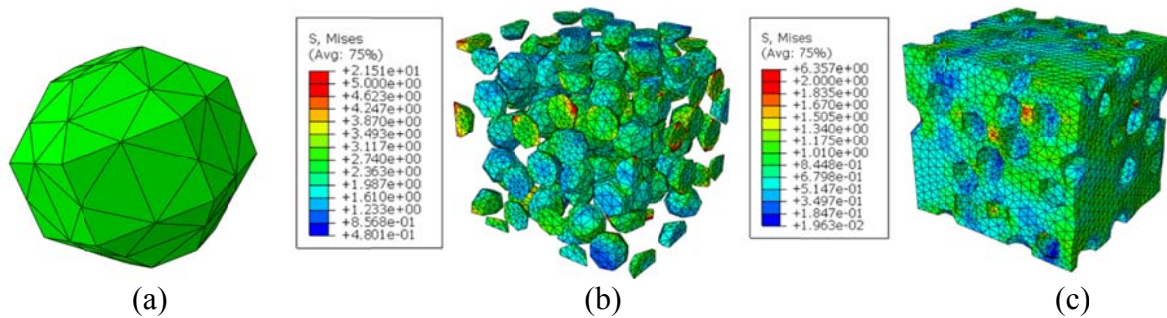


Fig. 3 (a) Icosahedron particle; (b) particle stresses and (c) matrix stresses

For effective stiffnesses, both particle and matrix are assumed as isotropic linear elastic materials having properties in Table 2. Particles are assumed to be SrAl_2O_4 stuffed tridymite (Yamada and Xu 2007). Under uniaxial tensile strain, stress distributions in particles and matrix are heterogeneous (Fig. 3(b)).

Table 2 Material properties

Matrix (EpoxAcast ® 690)		Particle (Yamada and Xu 2007)	
Young's modulus	3.94GPa	Young's modulus	102GPa
Poisson ratio	0.3	Poisson ratio	0.2

4.1 Two-Point Correlation Function Analysis

For a RVE with volume fraction of 0.25 and particle size of 2, TPCF were plotted in Fig. 4. The synthetic model was constructed by $75 \times 75 \times 75$ voxels. For all nine RVEs, TPCF were computed. The relationship in Eq. (2) is confirmed from this result.

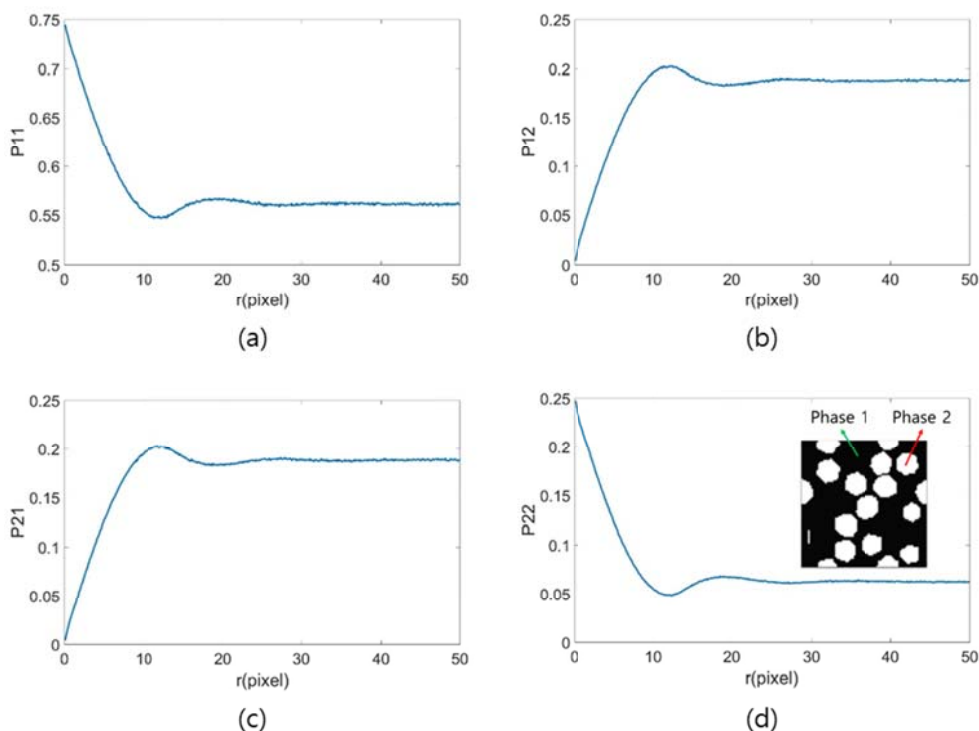


Fig. 4 TPCF for a synthetic RVE ($v_f=0.25$ and $D=0.35$)

4.2 Morphology Analysis

In order to increase the number of particles, ten RVEs with volume fraction of 0.25 and particle size of 2 were generated. Morphology analysis was conducted with 3D voxel-based images. Cubic RVE size 10 was divided by 75 voxels so the reference unit voxel size was 0.13333. The morphology analysis results were scaled by the unit voxel size. No specific probabilistic model for random generation of particles was assumed. Although the particle size is fixed to one value, smaller particles can also be generated to meet the specified volume fraction. Histograms of scaled results from ten morphology analyses are plotted in Fig. 5. Peak values of the volume, surface area, moment of inertia, principle radius, aspect ratio and shape index correspond to the specified size. Other values with small frequencies correspond to particles added to adjust the volume fraction. It is noteworthy that real SEM or CT images must be analysed by image processing to find out true probabilistic model of the microstructure feature.

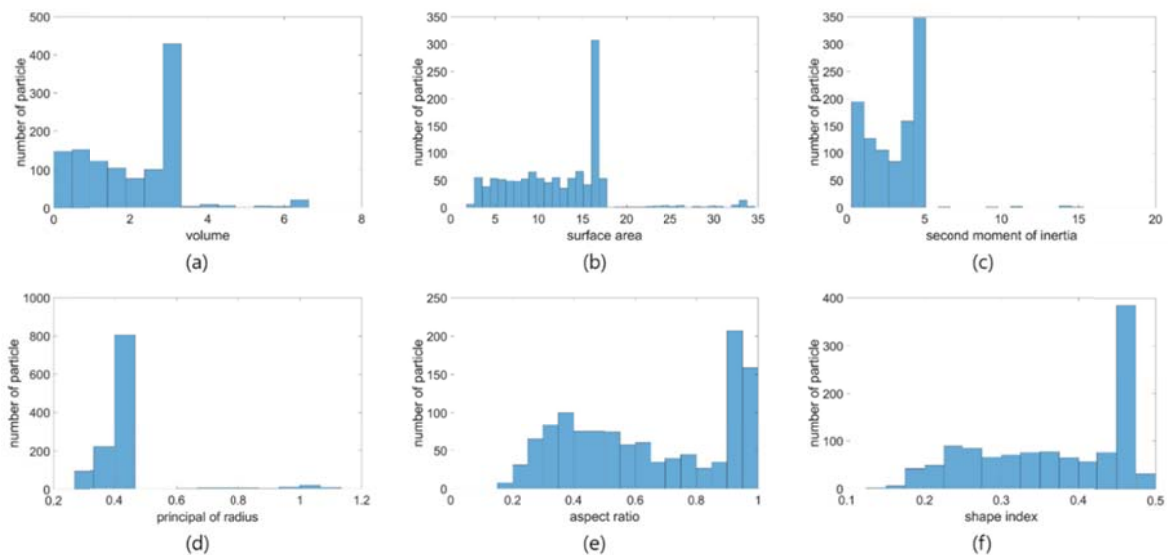


Fig. 5 Histogram of morphological parameters

4.3 Computational Homogenization for Effective Stiffness

Effective properties of all synthetic RVEs were obtained by the FE-based computational homogenization technique. Correlations of effective elastic properties with volume fraction and particle size are illustrated in Fig. 6.

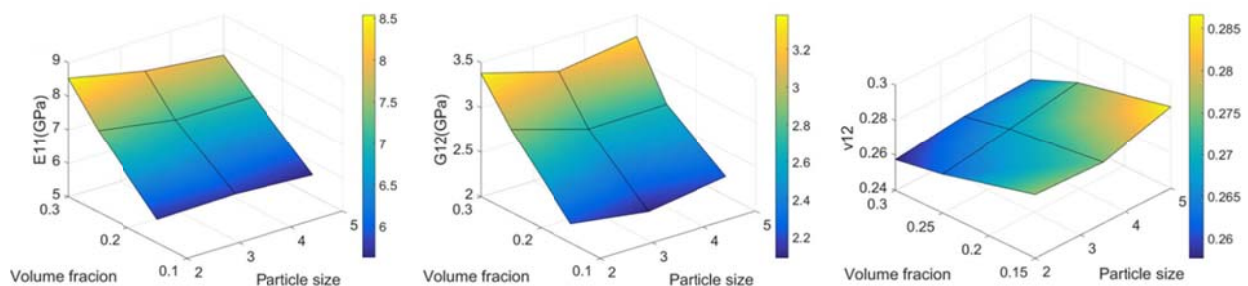


Fig. 6 Relationship between effective elastic properties (E_{11} , G_{12} and ν_{12}) with volume fraction and particle size

As the volume fraction increases, E_{11} and G_{12} show increasing tendency but ν_{12} shows slightly decreasing tendency but the variation appears marginal. However, particle size effect was not clear. To avoid biased results, it is desirable to conduct multiple RVE analyses for each of the nine RVEs.

5. CONCLUSIONS

In this paper, we demonstrated structure-property correlation analysis for particulate composites. TPCF was used as a statistical descriptor and morphological properties of particles were expressed in terms of various quantitative measures. Effective linear elastic properties were calculated by FE-based computational homogenization technique. Applying PBC is challenging for non-matching FE meshes on facing surface. Therefore, a numerical interpolation scheme was proposed to overcome the challenge. Varying the volume fraction and particle size, the structure-property correlation was evaluated. Noticeable changes of effective material properties were observed by varying the local volume fraction. The proposed microstructure analysis method will be a practical suite of analytical approaches and numerical tools for hierarchical design of composite materials.

ACKNOWLEDGMENT

This work was supported by Creative-Pioneering Researchers Program through Seoul National University (SNU). Authors are grateful for their supports.

REFERENCES

- Akpoymare, A.I., Okereke, M.I. & Bingley, M.S., 2017. Virtual testing of composites: Imposing periodic boundary conditions on general finite element meshes. *Composite Structures*, 160, 983-994.
- Charalambakis, N., 2010. Homogenization techniques and micromechanics. A survey and perspectives. *Applied Mechanics Reviews*, 63 (3).
- Fullwood, D.T., Niezgodá, S.R., Adams, B.L. & Kalidindi, S.R., 2010. Microstructure sensitive design for performance optimization. *Progress in Materials Science*, 55 (6), 477-562.
- Ghazavizadeh, A., Soltani, N., Baniassadi, M., Addiego, F., Ahzi, S. & Garmestani, H., 2012. Composition of two-point correlation functions of subcomposites in heterogeneous materials. *Mechanics of Materials*, 51, 88-96.
- Mcdowell, D.L. & Olson, G.B., 2008. Concurrent design of hierarchical materials and structures. *Scientific Modeling and Simulations*, 15 (1-3), 207-240.
- Olson, G.B., 1997. Computational design of hierarchically structured materials. *Science*, 277 (5330), 1237-1242.
- Shahzamanian, M.M., Tadepalli, T., Rajendran, A.M., Hodo, W.D., Mohan, R., Valisetty, R., Chung, P.W. & Ramsey, J.J., 2014. Representative volume element based modeling of cementitious materials. *Journal of Engineering Materials and Technology-Transactions of the Asme*, 136 (1).

- Teranishi, M., Kuwazuru, O., Gennai, S., Kobayashi, M. & Toda, H., 2016. Three-dimensional stress and strain around real shape si particles in cast aluminum alloy under cyclic loading. *Materials Science and Engineering a-Structural Materials Properties Microstructure and Processing*, 678, 273-285.
- Tewari, A., Gokhale, A.M., Spowart, J.E. & Miracle, D.B., 2004. Quantitative characterization of spatial clustering in three-dimensional microstructures using two-point correlation functions. *Acta Materialia*, 52 (2), 307-319.
- Torquato, S., 2002. *Random heterogeneous materials: Microstructure and macroscopic properties* New York: Springer.
- Xu, C., Gao, S.M. & Li, M., 2017. A novel pca-based microstructure descriptor for heterogeneous material design. *Computational Materials Science*, 130, 39-49.
- Xu, H.Y., Dikin, D.A., Burkhart, C. & Chen, W., 2014. Descriptor-based methodology for statistical characterization and 3d reconstruction of microstructural materials. *Computational Materials Science*, 85, 206-216.
- Yamada, H. & Xu, C.N., 2007. Ab initio calculations of the mechanical properties of SrAl_2O_4 stuffed tridymite. *Journal of Applied Physics*, 102 (12).
- Yuan, Z. & Fish, J., 2008. Toward realization of computational homogenization in practice. *International Journal for Numerical Methods in Engineering*, 73 (3), 361-380.